Trop J Nat Prod Res, November 2025; 9(11): 5739 - 5751
ISSN 2616-0684 (Print)
ISSN 2616-0692 (Electronic)

Tropical Journal of Natural Product Research

Available online at https://www.tjnpr.org

Original Research Article

# Molecular Docking Prediction and *In Vitro* Investigation of Polyphenol Fraction from *Senecio biafrae* on Pro-Inflammatory Enzymes

Funke T. Akinola[1], Joseph T. Apata[2]*, Mukaila B. Adekola[3], Felix O. Afolabi[4] and Olusegun O. Babalola[5]

[1]*Department of Biochemistry, College of Science and Engineering, Venite University, P.M.B. 002, Iloro Ekiti, Ekiti State, Nigeria*
[2]*Department of Biochemistry, Faculty of Natural and Applied Sciences, Hallmark University, KM 65, Sagamu-Ore, Expressway, P.M.B. 2016, Ijebu-Itele, Ogun State, Nigeria*
[3]*Department of Environmental Management and Toxicology, Federal University of Agriculture Abeokuta, P.M.B. 2240, Nigeria*
[4]*Department of Pharmacology, Federal University of Health Sciences, Ila-Orangun, P.M.B. 204, Ila-Orangun, Osun State, Nigeria*
[5]*Department of Biochemistry and Molecular Biology, Obafemi Awolowo University, P.M.B. 13, Ile-Ife, Nigeria*

ARTICLE INFO

*Article history:*
Received 24 December 2024
Revised 15 August 2025
Accepted 17 September 2025
Published online 01 December 2025



ABSTRACT

Plants containing anti-inflammatory compounds often regulate proinflammatory enzymes to prevent the onset of inflammatory conditions. This study aimed to examine the effect of *Senecio biafrae* leaf fractions on pro-inflammatory enzymes using *an in vitro* model, as well as molecular docking prediction technique to explore the anti-inflammatory properties of *Senecio biafrae* leaves. Thirty grams of *Senecio biafrae* crude extract were divided into two halves, with the first half partitioned and the second half fractionated using Amberlite XAD-16 resin to obtain polyphenol-rich fractions. The flavonoids and phenolic contents of the fractions were quantified. The polyphenol-rich fraction was fingerprinted using liquid chromatography mass spectrometry and evaluated for anti-proinflammatory enzyme activities. The compounds detected were subsequently analysed through molecular docking. The results indicated that the polyphenol-rich fraction had the highest total phenolic (1485.51±0.14 µg GAE/g) and flavonoid (428.07±0.03 µg QUE/g) concentrations. It also exhibited high xanthine oxidase activity in a dose-dependent manner and comparable lipoxygenase inhibitory activity with the standard anti-inflammatory drug. Comparing the polyphenol-rich fraction of *Senecio biafrae* to standard anti-inflammatory drugs, molecular docking analysis predicted that Fluperlapin and Methyl picraquassioside-A had the highest inhibitory activities against xanthine oxidase (-9.9 kcal/mol.) and cyclooxygenase (-8.9 kcal/mol.), while Stigmatellin Y had similar inhibitory activity against 5-lipoxygenase. *Senecio biafrae's* polyphenolic-rich fraction may serve as a foundation for the development of novel anti-inflammatory agents, but further research is needed to validate its anti-inflammatory properties through structural elucidation and *in vivo* investigation of the compounds identified in the polyphenol-rich fraction of *Senecio biafrae.*

**Keywords:** Antioxidant, Anti-inflammation, 5-Lipoxygenase, Cyclooxygenase-2, Molecular docking

## Introduction

Inflammation serves as a crucial physiological reaction to tissue damage, infection, or irritants. However, when inflammation becomes chronic or excessive, it can lead to the onset of various long-term diseases, including arthritis, heart conditions, and cancer.[1,2] This harmful impact is often caused by the overproduction of pro-inflammatory substances such as prostaglandins and leukotrienes, which are generated by enzymes like cyclooxygenase-2 (COX-2), 5-lipoxygenase, and xanthine oxidase (XO).[3]

*Corresponding author; Email: tjapata@hallmarkuniversity.edu.ng
Tel.: +234 813-3646-454

Citation Akinola, F T , Apata J T, Adekola M B, Afolabi F O , Babalola O O. Molecular Docking Prediction and *In vitro* Investigation of Polyphenol Fraction from *Senecio biafrae* on Pro-Inflammatory Enzymes. Trop J Nat Prod Res. 2025; 9(11): 5739 – 5751 https://doi.org/10.26538/tjnpr/v9i11.64

Official Journal of Natural Product Research Group, Faculty of Pharmacy, University of Benin, Benin City, Nigeria.

While non-steroidal anti-inflammatory drugs (NSAIDs) are frequently prescribed to manage inflammation, their prolonged use can lead to adverse effects, including gastrointestinal ulceration, kidney damaged, and cardiovascular risks.[4] As a safer alternative, attention has shifted toward the discovery of plant-derived compounds with anti-inflammatory potential. *Senecio biafrae* (SB) from the Asteraceae family, a succulent and leafy vegetable widely consumed in West Africa, is traditionally used for managing various health conditions. It is rich in micronutrients and secondary metabolites, including polyphenols and flavonoids, which have been associated with antioxidative, anti-diabetic, and fertility-enhancing effects.[5] Previous research has demonstrated that compounds found in SB exhibit inhibitory effects on metabolic enzymes, specifically α-amylase and α-glucosidase, underscoring their pharmacological relevance.[6] Nonetheless, there is limited knowledge regarding its possible inhibitory influence on proinflammatory enzymes. This study is novel in its approach to integrate bioactivity-guided phytochemical profiling with molecular docking analysis to predict potential anti-inflammatory compounds from SB. While prior research focused on its anti-diabetic and fertility-enhancing properties, this is the first study to systematically evaluate its polyphenol-rich fraction (PRF) for anti-inflammatory effects utilizing a dual *in vitro* and *in silico* strategy. The use of molecular docking further enhances the predictive value of the findings and provides a foundation for future structure-based drug design. This research seeks to explore the anti-inflammatory properties of PRF derived from SB leaves by

examining its inhibitory effects on particular pro-inflammatory enzymes and employing molecular docking techniques.

## Materials and Methods

*Plant Collection and Identification*

Freshly collected SB leaves were sourced in January 2024 from Akamo, Iperindo (Latitude: N07º29′40″; Longitude: E04º49′26″; Distance: 541 m), located in Osun State. The botanical specimen was classified and confirmed at the Ife Herbarium within the Department of Botany at Obafemi Awolowo University in Ile-Ife, Nigeria. The voucher specimen was deposited to the Herbarium with the identification code IFE-17936.

*Preparation of Plant Extract*

SB leaves were chopped into smaller pieces, properly cleaned with pure distilled water, and air-dried for two weeks. A mechanical grinding machine was utilized to compress the dried leaves into fine powder. The powdered plant sample (350 g) was steeped in ethanol at 25ºC for 72 hours. At 40°C, the ethanol extract was concentrated with the aid of a rotary evaporator (Edward Vacuum Corporation, Crawley, England). The crude ethanol extract was kept in the desiccator until additional processing was necessary.[6]

*Partitioning of SB Extract*

A 30g sample of SB extract was submerged in distilled water (200 ml), agitated well, and then filtered with the aid of Whatman Number 1 filter paper. Following filtration, the product obtained was sequentially extracted with 400 ml of absolute dichloromethane (DCM), ethyl acetate (EA), as well as methanol (MeOH). Each of the solvent fraction was vigorously stirred and allowed to form layers. The various solvent fractions were concentrated individually in the rotary evaporator of Edward High Vacuum Pump Cooperation in Crawley, England whereas the aqueous fraction (AQF) was reduced in volume prior to being lyophilized. After this process, the obtained fractions were weighed, tagged, as well stored in desiccators for future analysis. Three fractions were obtained: dichloromethane fraction (DCMF), ethyl acetate fraction (EAF), as well as aqueous fraction (AQF). However, AQF was discarded and not utilized in the course of research.[6]

*Preparation of Polyphenol-rich Fraction from* SB Plant

The fraction rich in polyphenols was extracted via an Amberlite XAD-16 resin column using a standard method.[7] Initially, a powdered (800 g) sample of the plant was macerated in acidified methanol [comprising 80% (v/v) methanol, 19% (v/v) $H_2O$, 1% (v/v) acetic acid] for a duration of 72 hours at 40°C, with periodic agitation. The mixture obtained was first filtered with the aid of filter paper (Whatman number 1) and then dried in a vacuum pressure utilizing a Buchi Rotavapor R-205 rotary evaporator (Switzerland) at 40°C. The extract was introduced onto the column using acidified water [(99% (v/v) $H_2O$, 1% (v/v) acetic acid], followed by a wash with the same solvent. Elution was performed using a solvent mixture consisting of 80% (v/v) ethanol, 19.9% (v/v) $H_2O$, as well as 0.1% (v/v) trichloroacetic acid. The eluates collected were concentrated via vacuum pressure at 37 °C with a Buchi Rotavapor R-205 rotary evaporator (Switzerland) and lyophilized to obtain PRF. The PRF percentage yield was mathematically determined from the plant starting materials via Equation 1 provided below:

$$\text{Yield (\%)} = 1 - \frac{LF}{DL} \times 100 \quad \text{---------- Equation 1}$$

Where LF= weight of lyophilized fraction (g), DL = weight of the sample extracted (g)

*Estimation of Total Phenolics*

Spectrophotometry was utilized to assess the total phenolic content of SB fractions via a standard procedure.[8,9] To establish a standard curve, various volumes of a gallic acid solution (0.01 mg/ml) were pipetted into separate test tubes at 0, 20, 40, 60, 80, and 100 µL. Each test tube was then filled with distilled water, reaching a total volume of 1 mL, followed by the addition of 200 µL of Folin–Ciocalteu's phenol reagent. After allowing the mixture to incubate for 15 minutes at room temperature, 1 mL of a 7% (w/v) sodium carbonate solution ($Na_2CO_3$) was incorporated. The samples were subsequently incubated for an additional 1.5 hours under the same temperature conditions.

The absorbance was taken using a UV-Visible Spectrophotometer (S23A, ESCHMED Medical, England) at 750 nm. For analyzing the SB extract, a sample (1 mg/ml) of 100 µL was added to distilled water (900 µL) and 10% (v/v) Folin–Ciocalteu's reagent (200 µL). This mixture was incubated for 15 minutes at 25ºC and mixed with 7% (w/v) $Na_2CO_3$ solution (1mL), followed by a further incubation of 1.5 hours. Each trial was performed in triplicate, and the absorbance was recorded at 750 nm. The amount of phenolic compounds was assessed by interpolating the absorbance values from the gallic acid calibration plot. This measurement was reported in milligrams of gallic acid equivalents for each gram of extract (mg GAE/g extract).

*Estimation of Total Flavonoids*

In accordance with established protocols, spectrophotometry was employed to measure the flavonoid levels in the SB fractions. A calibration curve was created by adding 0, 20, 40, 60, 80, and 100 µL of a quercetin solution (0.01 mg/mL) to test tubes, adjusting the total volume with distilled water to 100 µL. Subsequently, 25 µL of a 5% (w/v) sodium nitrite ($NaNO_3$) solution was introduced into each tube, and the mixtures were incubated at 25ºC for 5 minutes.

The colorimetric reaction commenced with the addition of 50 µL of 2 M sodium hydroxide (NaOH) as well as 25 µL of 10% (w/v) aluminium chloride ($AlCl_3$). After incubating for another 15 minutes at 25ºC, their absorbance was measured at a wavelength of 510 nm. For the analysis of samples, 100 µL of the SB extract (1 mg/mL) was added to 100 µL of distilled water and 5% (w/v) $NaNO_3$ (25 µL), followed by a five-minute incubation at 25°C. The subsequent addition of 50 µL of 2 M NaOH and 25 µL of 10% $AlCl_3$ was done, and the blend was incubated for a further 15 minutes. The absorbance was recorded via a UV-Visible Spectrophotometer (S23A ESCHMED Medical, England) at 510 nm. A calibration graph was produced by correlating the quercetin mass (mg) to absorbance (nm) to ascertain the total flavonoid concentration in the SB fractions. This measurement was reported in milligrams of quercetin equivalents for gram of extract (mg QE/g extract).[10,11]

*Lipoxygenase (LOX) Inhibitory Assay*

According to the previously described procedure, linoleic acid was used as the substrate for a spectrophotometric evaluation of PRF ability to inhibit lipoxygenase.[12] Quercetin, when dissolved in the same buffer, acted as the standard reference inhibitor. A stock of PRF's solution was created at 1 mg/mL in phosphate buffer. The assay was comprised of a test sample varying between 0.1 and 0.5 mg/mL, 50 µL of lipoxygenase solution (0.28 U/mL), and 150 µL of phosphate buffer (0.0667 M, pH 7.5).

The enzymatic reaction commenced with the introduction of 250 µL of linoleic acid (0.15 mM) buffer solution. The increase in absorbance at 234 nm, measured by a UV-Visible Spectrophotometer (S23A ESCHMED Medical, England), was monitored over a two-minute period to indicate enzyme activity. A 1% (v/v) methanol solution lacking PRF served as the negative control. The % inhibition of PRF was determined via Equation 2.

$$\text{Inhibition (\%)} = 1 - \frac{B}{A} \times 100 \quad \text{---------- Equation 2}$$

The absorbance change of the test conducted with the PRF is shown in Equation B, whereas the absorbance change of the test conducted without the PRF, which acts as the negative control, is shown in Equation A.

*Xanthine Oxidase (XO) Inhibitory Assay*

According to earlier research, a spectrophotometric technique was used to assess the PRF's inhibitory effect on xanthine oxidase using xanthine as the substrate.[12,13] A stock solution of PRF was created using a phosphate buffer, achieving 1 mg/ml. For the positive control, allopurinol was also diluted in the same buffer. The reaction mixture contained 150 µL of phosphate buffer (0.0667 m, pH 7.5), combined with 50 µL of the test sample (ranging from 0.1 to 0.5 mg/ml) as well as 50 µL of xanthine oxidase solution (0.28 u/mL). The reaction was initiated by adding 250 µL of xanthine substrate solution, which had a concentration of 0.15 mM in the buffer. By utilizing a UV-

Visible spectrophotometer (S23A, ESCHMED Medical, England) to measure the formation of uric acid, as indicated by an increase in absorbance at 295 nm during a 2-minute period, enzymatic activity was monitored. In this case, the negative control was phosphate buffer. Equation 3 was adopted to interpolate the percentage of xanthine oxidase activity inhibition.

Inhibition (%) = $1 - \frac{B}{A} \times 100$ ---------- Equation 3

In Equation 3, A denotes the variation in absorbance of the reaction mixture that contains the PRF, while B signifies the change in absorbance of the reaction mixture that does not include the PRF, serving as the negative control. The xanthine oxidase % inhibition was utilized to assess the enzyme's inhibitory effect.

*LC–MS Profiling of PRF of SB Plant*

To attain clarity and purity, the PRF of SB was separately filtered via 0.45 µm as well as 0.2 µm membrane filters after being diluted with distilled ethanol to a concentration of 10 mg/ml. A working solution of 1 mg/ml was made by mixing 1.8 mL of double-distilled water with 200 µL of the filtered 10 mg/ml PRF. A dual electrospray ionization (ESI) source-equipped Agilent 1290 Infinity LC system was used to profile metabolites, including primary and secondary metabolites, utilizing an Agilent 6520 Accurate-Mass Q-TOF mass spectrometer. A 2.1 mm × 150 mm, 3.5 µm particle size, Agilent Zorbax Eclipse XDB-C18 narrow-bore column was used for the chromatographic separation. We kept the autosampler set at 4 °C as well as the column temperature at 25 °C. The mobile phase was a 60:40 (v/v) mixture of acetonitrile and water that was delivered at a rate of 0.5 milliliters per minute. PRF solution (3.0 µL) was added to the LC-MS device. With nitrogen serving as the collision gas and a fragmentor voltage of 125 V, data was gathered utilizing both positive and negative ionization modes. Data was collected in 1.03 seconds using the mass spectrometer in positive ion ESI mode, scanning a range of 100-3200 m/z.

In order to identify metabolites, the gathered LC-MS spectrum data was compared to entries in the METLIN database. Agilent Mass Hunter Qualitative Analysis software (version B.05.00) was used for peak detection and integration. [14,15]

*Molecular Docking Analysis*

*Ligand Preparation*

Ligands were prepared as earlier described in the literature.[15] The structural data files (SDF) of the phytochemicals identified from the PRF of *SB* leaves via LC-MS analysis, along with those of the reference compounds—Celecoxib, Licofelone, and Allopurinol—were obtained from the PubChem database (https://pubchem.ncbi.nlm.nih.gov/). These SDF compounds were imported into PyRx software (version 8, Windows platform) and subsequently converted to PDBQT format using the integrated Open Babel plugin. Prior to molecular docking, energy minimization was performed on all ligands to generate their optimized conformations for accurate docking analysis.

*Protein Preparation*

The crystal structures of Cyclooxygenase-2 (COX-2), 5-Lipoxygenase (5-LOX), as well as Xanthine Oxidase (XO) were retrieved from the Research Collaboratory for Structural Bioinformatics (RCSB) Protein Data Bank (https://www.rcsb.org/). The protein structures, in PDB format, were imported into UCSF Chimera version 1.14, for preprocessing. Non-standard residues, including water molecules, bound ligands, and metal ions, were initially removed to ensure structural integrity. Protein structure minimization was conducted via Chimera's structure editing tools, applying 100 steps of steepest descent (step size: 0.02 Å), followed by 10 steps of conjugate gradient minimization (step size: 0.02 Å), with updates every 10 intervals. Further preprocessing involved the removal of solvents, addition of hydrogen atoms, and assignment of partial atomic charges using the Gasteiger force field. Histidine residues were adjusted to reflect the appropriate protonation state. Additionally, modified residues were standardized by converting selenomethione (MSE) to methionine (MET), Bromo-UMP (5BU) to uridine monophosphate (UMP, U), methylselennyl-DUMP (UMS) to UMP (U), and methylselenyl-DCMP (CSL) to cytidine monophosphate (CMP, C). The fully prepared and energy-minimized protein structures were then exported and uploaded into PyRx software for molecular docking studies.[15]

*Docking Grid Space*

Molecular docking of the prepared protein as well as ligand structures was carried out using the AutoDock wizard integrated within the PyRx software environment (version 8 for Windows). Grid box size x: -3.3358, y: -23.5241, Z: 73.0239 and grid centre dimensions x: 65.6864 Å, y: 57.5041 Å, z: 77.4687 Å were set for COX-2 with the PDB ID of 5W58; grid box sizes x: 8.7183, y: 22.4773, z: 1.2559 and grid centre dimension x: 68.1346 Å, y: 59.4066 Å, z: 94.0178 Å were set for 5-LOX with PDB ID 3O8Y and grid box size x: 39.5719, y: 54.5950, z: 92.2164 and grid centre x: 66.5156 Å, y: 46.7911 Å and z: 50.2159 Å were set for OX with PDB ID 1FIQ. Three-dimensional (3D) visualizations of the protein–ligand complexes, along with two-dimensional (2D) representations of the molecular interactions, were generated using Discovery Studio Visualizer 2021 (version 21.1.0.20289).[15]

*Statistical Analysis*

The results of the experiment were shown as mean ± standard error of the mean (SEM) and analyzed using Microsoft Excel (Microsoft Office Suite, Excel version 2021 for Windows, USA) and GraphPad InStat software (version 5, GraphPad Software Inc., USA). For multiple comparisons, Tukey's post hoc test was used after one-way analysis of variance (ANOVA) to generate the statistical level of significance. Statistical significance of the observed variation was established at a threshold p-value of $< 0.05$.

## Results and Discussion

*Phytochemical composition of SB fractions*

Figures 1 and 2 show the summary of phenolic and flavonoid contents present in PRF, DCMF, MeOHF and EAF obtained from SB extract. Among these fractions, PRF exhibited the highest total phenolics ($1485.51 \pm 0.14$ µg GAE/g) and total flavonoids ($428.07 \pm 0.03$ µg QE/g) contents, suggesting its ability to act as a rich source of antioxidants. The EAF showed moderate phenolic content ($479.87 \pm 0.01$ µg GAE/g) and high flavonoid concentrations ($357.80 \pm 0.04$ µg QE/g), indicating therapeutic potential despite lower phenolics concentration. Comparatively, the DCMF and MeOHF fractions showed significantly lower contents of both phenolics and flavonoids. The phenolic as well as flavonoid contents of the SB leaf were found in the following increasing order: MeOHF<DCMF<EAF<PRF. It is clear that bioactive molecules with antioxidant properties are abundant in PRF and EAF fractions. This outcome is in line with other research results in the field.[16,17]

*Anti-inflammatory Activity of SB fractions*

*Xanthine oxidase activity*

The summary of the *in vitro* assessment of the inhibitory activity of PRF against xanthine oxidase is shown in Figure 3. The results showed varying degrees of PRF percentage inhibitory activities ranging from 80.79% to 93.95%. A dose dependent significant increase in xanthine oxidase inhibitory activity of PRF was observed from 0.1 to 0.5 mg/ml. PRF exhibited the highest percentage inhibitory activity (93.95 ± 0.67%) at 0.5 mg/ml when compared with the standard anti-inflammatory drug (allopurinol). Xanthine oxidase has been implicated in uric acid formation and the production of free

ISSN 2616-0684 (Print)
ISSN 2616-0692 (Electronic)

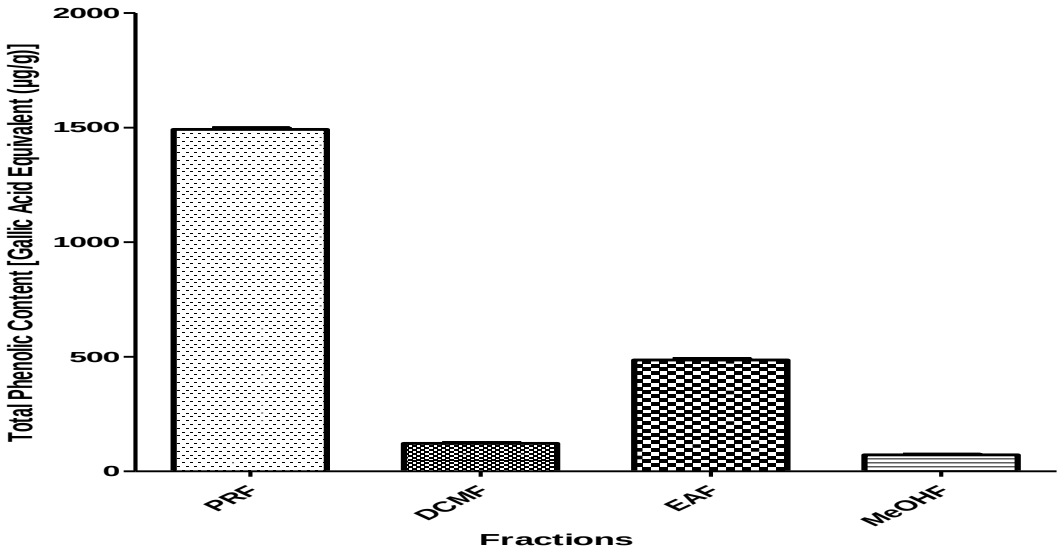


**Figure 1:** Total Phenolic Contents Contained in S.B Plant

Data were expressed as mean ± S.E.M. (n = 3). Means with different values are significantly different ($p < 0.05$). PRF: Polyphenol-rich fraction, DCMF: Dichloromethane fraction, EAF: Ethyl acetate fraction, MeOHF: Methanol fraction

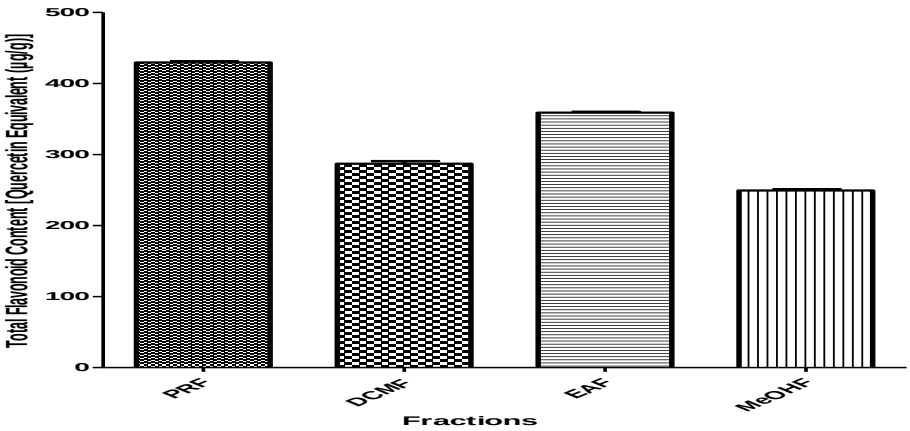


**Figure 2:** Total Flavonoid Contents Contained in S.B Plant

Data were expressed as mean ± S.E.M. (n = 3). Means with different values are significantly different ($p < 0.05$). PRF: Polyphenol-rich fraction, DCMF: Dichloromethane fraction, EAF: Ethyl acetate fraction, MeOHF: Methanol fraction

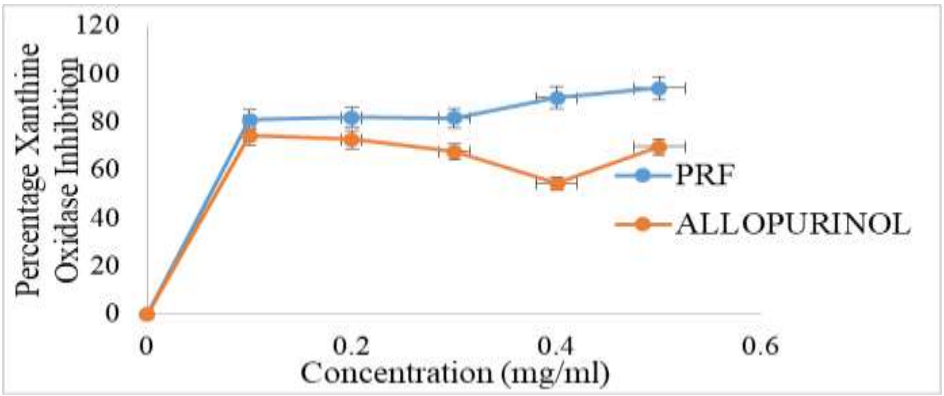


**Figure 3:** Effect of PRF of SB on *in vitro* Inhibition of Xanthine Oxidase

Data were expressed as mean ± S.E.M. (n = 3). Means with different values are significantly different ($p < 0.05$). PRF: Polyphenol-rich fraction, DCMF: Dichloromethane fraction, EAF: Ethyl acetate fraction, MeOHF: Methanol fraction

ISSN 2616-0684 (Print)
ISSN 2616-0692 (Electronic)

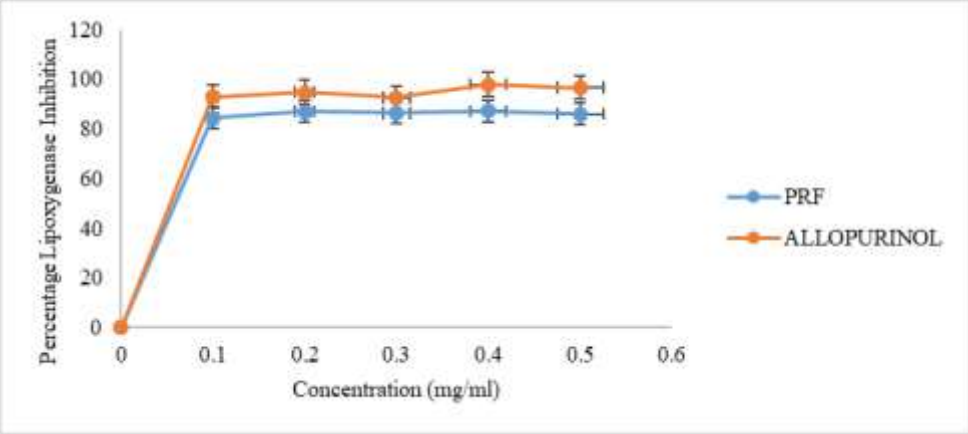


**Figure 4:** Effect of PRF of SB on *in vitro* Inhibition of Lipoxygenase

Data were expressed as mean ± S.E.M. (n = 3). Means with different values are significantly different ($p < 0.05$). PRF: Polyphenol-rich fraction, DCMF: Dichloromethane fraction, EAF: Ethyl acetate fraction, MeOHF: Methanol fraction

radicals, which could subsequently trigger the development of severe gout.[18,19] It has been reported that *Syzygium cumini* inhibits xanthine oxidase activity.[20] Inhibiting xanthine oxidase activity by fractions of SB especially PRF reduces uric acid synthesis, suggesting potential use for treating gout and hyperuricemia due to polyphenol's free radical scavenging properties.

*Lipoxygenase activity*

Figure 4 displays the inhibitory effect of PRF fractionated from SB against lipoxygenase. The results showed that the PRF fractionated from SB extract exhibited a moderate, concentration-dependent enzyme inhibition ranging from 84.51 ± 0.84% at 0.1 mg/ml to 87.27 ± 1.42% at 0.4 mg/ml. The highest inhibition was observed at 0.4 mg/ml, but the differences among these concentrations were not strictly dose-dependent. Notable variances were found between the rates of inhibition at different concentrations, with the 0.2 mg/ml concentration (87.09 ± 2.45%) and 0.4 mg/ml concentration (87.27 ± 1.42%) showing significantly higher activity compared to other concentrations tested ($p < 0.05$). Interestingly, lipoxygenase inhibition slightly decreased at 0.5 mg/ml (86.10 ± 0.15%), suggesting potential saturation or interference at higher concentrations. In contrast, quercetin, the reference standard, exhibited significantly ($P < 0.05$) higher lipoxygenase inhibitory activity across all concentrations studied (92.63 ± 2.82 to 97.91±0.47%). The maximum inhibitory activity (97.91±0.47%) was recorded at 0.4 mg/ml, significantly higher than that of PRF obtained from SB extract at the same concentration. The lipoxygenase pathway plays a crucial role in the immune response by oxidizing fatty acids to produce leukotrienes and other pro-inflammatory mediators. Compounds that inhibit lipoxygenase are valuable as anti-inflammatory agents. The PRF of SB, with significant inhibition, may contain bioactive compounds such as flavonoids and phenolics, which could be responsible for modulating LOX activity. While the PRF did not surpass quercetin in terms of inhibition, its consistently high inhibition across all concentrations suggests its potential as a natural anti-inflammatory agent. This supports previous findings on the antioxidant and anti-inflammatory properties of SB and aligns with its traditional use in managing inflammatory conditions.[21]

*Identification of bioactive compounds from PRF of SB through liquid chromatography-mass spectrometry (LC-MS).*

Liquid chromatography-mass spectrometry (LC-MS) is a hyphenated technique consisting of chromatography and a mass spectrometer. The primary focus of this technique is to analyse and separate mixtures of compounds in order to enhance their identification. To identify each compound in a mixture, LC-MS considers factors such as retention time (RT), molecular formulas, masses, peak area and chemical classification, especially for polar compounds. In this study, the PRF fractionated from SB was analysed using LC-MS. The analysis resulted in the identification of twenty bioactive compounds (Table 1). The mass spectrum and chromatogram of the identified compounds are shown in Figure 5. These compounds belong to diverse phytochemical classes, including alkaloids, phenolics, flavonoids, sesquiterpenes, glycosides, and organic aromatic compounds, which are known to have various pharmacological effects.[22] The presence of 2(1H)-quinolinone as an alkaloid suggests possible antimicrobial and neuroprotective potential, based on the reported biological activities of quinolinone derivatives.[23] Methyl picraquassioside A and glucocaffeic acid, both phenolic glycosides, are potent antioxidants that may contribute to the fraction's observed radical scavenging capacity in previous studies.[24] These phenolic compounds likely enhance the redox balance by neutralizing reactive oxygen species (ROS). Flavonoids identified, including allicin and 7-hydroxy-2',4',5'-trimethoxy isoflavone, are known for their anti-inflammatory, anticarcinogenic, and enzyme inhibitory properties, particularly against oxidase enzymes like xanthine oxidase and lipoxygenase.[25] This aligns with previous reports of enzyme inhibition by PRF of *S*B, suggesting that these flavonoids play a significant role in its therapeutic effects.[26] Trans-2,3-dihydroxy and hydroxyacetophenone, classified as polyphenols and phenols respectively, are known for their strong metal-chelating and radical-scavenging abilities. Additionally, salicylaldehyde, a simple phenolic compound, contributes to anti-inflammatory activity and may modulate prostaglandin pathways. Compounds such as stigmatellin γ (a chromone derivative) and fluperlapine (a benzazepine) are structurally complex and have pharmacological significance. Stigmatellin, has been linked to electron transport chain inhibition in microbial systems, suggesting potential antimicrobial activity. Fluperlapine, a tricyclic compound, exhibits antipsychotic and dopamine-modulating actions, which may explain part of its observed neuroprotective potential.[27] The detection of fatty acyl glycosides (e.g., hexanol arabinosyl glucoside) and auxin a, a plant growth hormone with structural similarity to lipid signaling molecules, suggests potential membrane-modulatory or signaling effects. Similarly, valiolone, a cyclitol, is structurally related to antidiabetic agents like voglibose, indicating a possible role in modulating carbohydrate metabolism. Interestingly, N-phenylacetyl aspartic acid and phenylacetonitrile are small aromatic and amino acid derivatives, with known roles in metabolic pathways and cell signaling.[28] The identification of alpha-(p-methoxyphenyl)-6-methyl-2-pyridineacrylic acid, although rare, suggests anti-inflammatory or antioxidant potential based on its structural resemblance to bioactive pyridines.[29]

*Molecular Docking Analysis*

**ISSN 2616-0684 (Print)**
**ISSN 2616-0692 (Electronic)**

Molecular docking analysis is a computer technique that predicts the best orientation of a tiny molecule when attached to a target protein.

| S/N | Compound Name | Formula | Mass | RT | Compound Class |
|---|---|---|---|---|---|
| 1 | (1H) Quinolinone | $C_9H_7N$ | 145.05 | 4.86 | Alkaloid |
| 2 | 1ethyl picraquassioside A | $C_{19}H_{24}O_{10}$ | 412.14 | 9.78 | Phenolics glycosides |
| 3 | ilucocaffeic acid | $C_{15}H_{18}O_9$ | 342.09 | 8.68 | Phenolics |
| 4 | rans-2,3-Dihydroxy | $C_9H_7O_4$ | 179.15 | 6.45 | Polyphenol |
| 5 | Allicin | $C_{12}H_{18}O_4$ | 226.12 | 8.29 | Flavonoid |
| 6 | Hydroxyacetopherone | $C_8H_8O_2$ | 136.05 | 6.24 | Phenol |
| 7 | Salicylaldehyde | $C_7H_6O_2$ | 122.04 | 5.43 | Organic |

**Table 1:** Identification of Bioactive Compounds through LC-MS from PRF of SB

RT: Retention Time

| | | | | | |
|---|---|---|---|---|---|
| | | | | | aromatic |
| 8 | (3',4,'5'-Trihydroxy Phenyl)-gamma Valerolactone | $C_{11}H_{12}O_5$ | 224.07 | 8.10 | Phenolic - |
| 9 | Phenylacetonitrile | $C_8H_7N$ | 117.06 | 7.83 | Organic |
| 10 | Methylbenzaldehyde | $C_8H_8O$ | 120.06 | 7.09 | Benzenoid |
| 11 | Sterebin D | $C_{18}H_{30}O_3$ | 294.22 | 17.47 | Sesquiterpene |
| 12 | 3-oxo-3-phenyl Propanoate | $C_9H_8O_3$ | 164.05 | 6.64 | Phenyl ketone |
| 13 | Stigmatellin γ | $C_{29}H_{40}O_6$ | 484.28 | 21.27 | Chromones |
| 14 | Fluperlapine | $C_{19}H_{20}FN_3$ | 309.4 | 14.42 | Benzazepine |
| 15 | N-phenylacetyl aspartic Acid | $C_{12}H_{13}NO_5$ | 251.08 | 6.56 | - Aspartic acid |
| 16 | 7-hydroxy-2', 4', 5'tri methoxy isoflavone | $C_{18}H_{16}O_6$ | 328.09 | 6.91 | Flavonoid - |
| 17 | Hexanol arabinosyl Glucoside | $C_{17}H_{32}O_{10}$ | 396.19 | 7.51 | Fatty acyl Glycosides |
| 18 | Alpha- (p-methoxy phenyl) -6-methyl-2-pyridineacrylic acid | $C_{16}H_{15}NO_3$ | 269.11 | 14.19 | - |
| 19 | Auxin a | $C_{18}H_{32}O_5$ | 328.23 | 14.07 | Carbocyclic |
| 20 | Valiolone | $C_7H_{12}O_6$ | 192.06 | 1.26 | Cyclitol |

It aids in determining binding affinity and interaction processes, which are crucial in drug development, biochemical research, and molecular biology. Compounds detected in the PRF of SB by LC-MS were analysed through molecular docking studies with standard anti-inflammatory drugs (Celecoxib, Licofelone, Allopurinol). The study's findings, as indicated by Gibb's free energy (ΔG) in Table 2, revealed a range of binding affinities for the protein targets (COX- 2, 5-LOX, OX). Methyl Picraquassioside A, Stigmatellin Y and Fluperlapin exhibited the highest binding affinities for COX-2 (-8.9 Kcal/mol), 5-LOX (-7.7 Kcal/mol) and OX (-9.9 Kcal/mol) compared to the standard ligands (Table 2). Biovia Discovery Studio 2021 showed that Methyl picraquassioside A (CID: 85363137), Fluperlapin (CID: 49381) and Stigmatellin Y (CID:5282078) interacted with specific active site amino acid residues of COX-2, 5-LOX and OX respectively (Figure. 6, Figure 7 and Figure 8) similar to the standard drug but with different bonds (Figure 9, Figure 10 and Figure 11). Additionally, the docking simulation of Methyl picraquassioside A (CID: 853631337) with COX-2 (PDB ID: 5W58) showed strong interactions. Methyl picraquassioside A formed conventional hydrogen bonds with amino acid residues such as GLU465, and GLN 42, as well as carbon hydrogen bond interactions involving CYS41 and CYS 47. Methyl picraquassioside A also utilized carbon hydrogen bond to interact with CYS 41 and CYS 47, Pi-Donor hydrogen bond with TRY 130 and ASP 125, Alky bond with PRO 153, ARG 44 and Pi-Alkyl bond with CYS 36 and ARG 44 (Figure 6). The three dimensional (3D) model shows that Methyl picraquassioside A was deeply buried within the COX-2 active site, suggesting significant potential for COX-2 inhibition. This observation was consistent with an earlier report.[30] Stigmatellin Y

**Table 2:** Binding Affinities of Bioactive Compounds Identified from PRF of SB Leaves and Standard Inhibitor for Anti- Inflammatory Protein Target

| S/N | Compounds Name | PubChem CID | ΔG Energy (Kcal/mol.) | | |
|---|---|---|---|---|---|
| | | | COX-2 | 5-LOX | OX |
| 1 | 2(1H) Quinolinone | 6038 | -7.2 | -6.6 | -6.9 |
| 2 | Methyl picraquassioside A | 85363137 | -8.9 | -6.4 | -8.7 |
| 3 | Glucocaffeic Acid | 6148082 | -8.6 | -7.2 | -8.4 |
| 4 | Trans-2,3-Dihydroxycinnamate | 5282146 | -6.7 | -7.3 | -6.5 |
| 5 | Allicin | 86374 | -6.3 | -6.5 | -6.4 |

**ISSN 2616-0684 (Print)**
**ISSN 2616-0692 (Electronic)**

| | | | | | |
|---|---|---|---|---|---|
| 6 | Hydroxyacetopherone | 7469 | -6.2 | -6.4 | -5.9 |
| 7 | Salicylaldehyde | 6998 | -5.9 | -5.8 | -5.3 |
| 8 | (3',4',5'-Trihydroxy phenyl)-gamma Valerolactone | 92850118 | -7.5 | -6.8 | -7.4 |
| 9 | Phenylacetonitrile | 8794 | -5.7 | -5.4 | -5.7 |
| 10 | Methylbenzaldehyde | 12105 | -6.0 | -5.8 | -5.6 |
| 11 | Sterebin D | 14396288 | -6.6 | -7.0 | -7.3 |
| 12 | 3-oxo-3-phenylpropanoate | 9543196 | -6.6 | -6.8 | -6.7 |
| 13 | Stigmatellin Y | 5282078 | -7.6 | -7.7 | -8.1 |
| 14 | Fluperlapin | 49381 | -8.6 | -7.3 | -9.9 |
| 15 | N-phenylacetyl aspartic acid | 13958181 | -6.4 | -6.4 | -7.5 |
| 16 | 7-hydroxy-2',4',5' trimethoxyisoflavone | 15337591 | -8.5 | -7.1 | -8.7 |
| 17 | Hexanol arabinosyl glucoside | 131751182 | -7.9 | -6.7 | -7.4 |
| 18 | (p-methoxy phenyl)-6-methyl-2- pyridineacrylic acid | 6300471 | -8.3 | -7.5 | -7.8 |
| 19 | Auxin a | 92772 | -7.7 | -6.2 | -8.3 |
| 20 | Valiolone | 443630 | -5.8 | -6.4 | -6.5 |
| S/N | Standard Inhibitor | | | | |
| 1 | Celecoxib | 2662 | -8.5 | | |
| 2 | Licofelone | 133021 | | -7.9 | |
| 3 | Allopurinol | 135401907 | | | -5.8 |

(CID: 5282078) showed notable binding within the active site of 5-LOX (PDB ID: 3O8Y). Multiple interactions were recorded, including van der Waals forces and pi-alkyl interactions, indicating hydrophobic stabilization (Figure 7). Hydrogen bonds with residues near the iron-binding domain of 5-LOX suggest that Stigmatellin Y may interfere with leukotriene synthesis, supporting its potential anti-inflammatory activity. This finding was consistent with previous report on the inhibition of lipoxygenase activity by *Siphonochilus aethiopicus*.[31] Figure 8 showed the binding interaction between Fluperlapin **a**nd OX**,** a key enzyme involved in purine metabolism and the production of uric acid. The 3D (left) and 2D (right) models display how Fluperlapin is situated within the enzyme's active site. The docking analysis revealed that Fluperlapin fits well within the xanthine oxidase binding pocket, stabilized by a network of hydrogen bonds, hydrophobic forces, and pi-interactions. Conventional hydrogen bonds (CYS 47 and TRY130) were observed between Fluperlapin and critical polar residues, anchoring the ligand in a favorable conformation. pi–alkyl interactions (CYS 36, ALA 156, PRO 153, SER 49 and GLY 135) occurred with aromatic residues within the active site, suggesting enhanced binding affinity through pi-electron cloud overlap—typical of ligands with aromatic moieties. Van der Waals interactions contributed to additional stabilization with surrounding residues like GLY 461, ASN 839, MET 48, PRO 154, VAL 155. The interaction pattern indicates that Fluperlapin is likely positioned near the molybdenum cofactor site**,** where xanthine conversion to uric acid takes place, suggesting possible inhibition of enzyme catalysis. The findings of this current study were in concordance with the previous report.[31] Figure 9 displays the molecular interaction between Celecoxib (CID: 2662) and cyclooxygenase-2 (COX-2, PDB ID: 5W58) using 3D and 2D models. In the 3-dimensional structure (left), Celecoxib is observed binding strongly within the COX-2 active site pocket, surrounded by structurally

significant residues such as HIS 133, TYR136, ALA156, ASP157, and GLN461. The active site adopts a deep, hydrophobic groove composed of α-helices, β-sheets, and loops, which provide a favorable environment for the ligand. The 2-dimensional interaction (right) highlights the

ISSN 2616-0684 (Print)
ISSN 2616-0692 (Electronic)

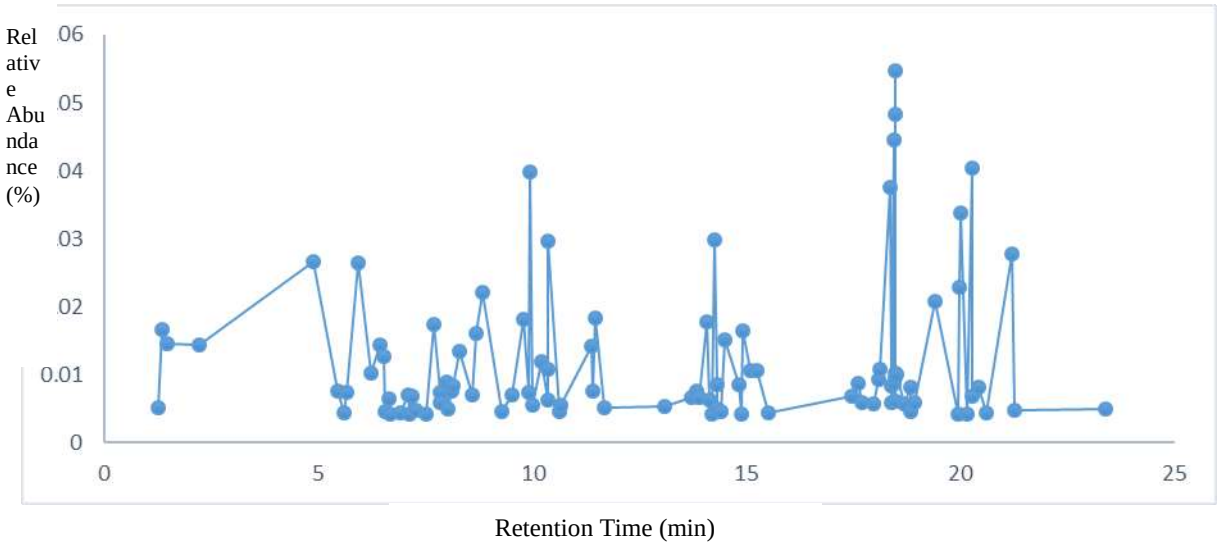


**Figure 5:** Chromatogram of identified compounds from PRF of SB

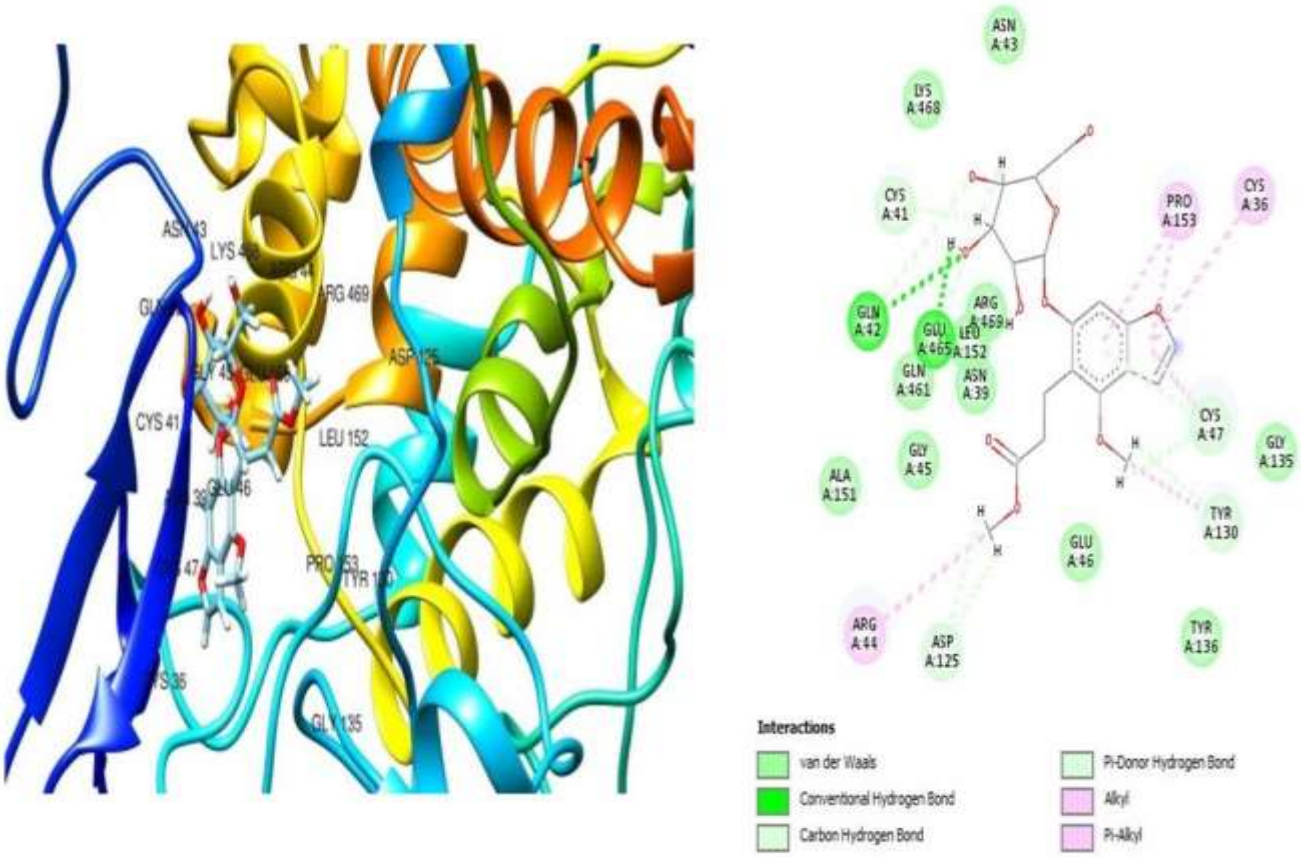


**Figure 6:** Molecular interaction of amino acids residues of COX-2 (PDB ID: 5W58) with Methyl picraquassioside A (CID: 853631337), 3D left, 2D right

ISSN 2616-0684 (Print)
ISSN 2616-0692 (Electronic)

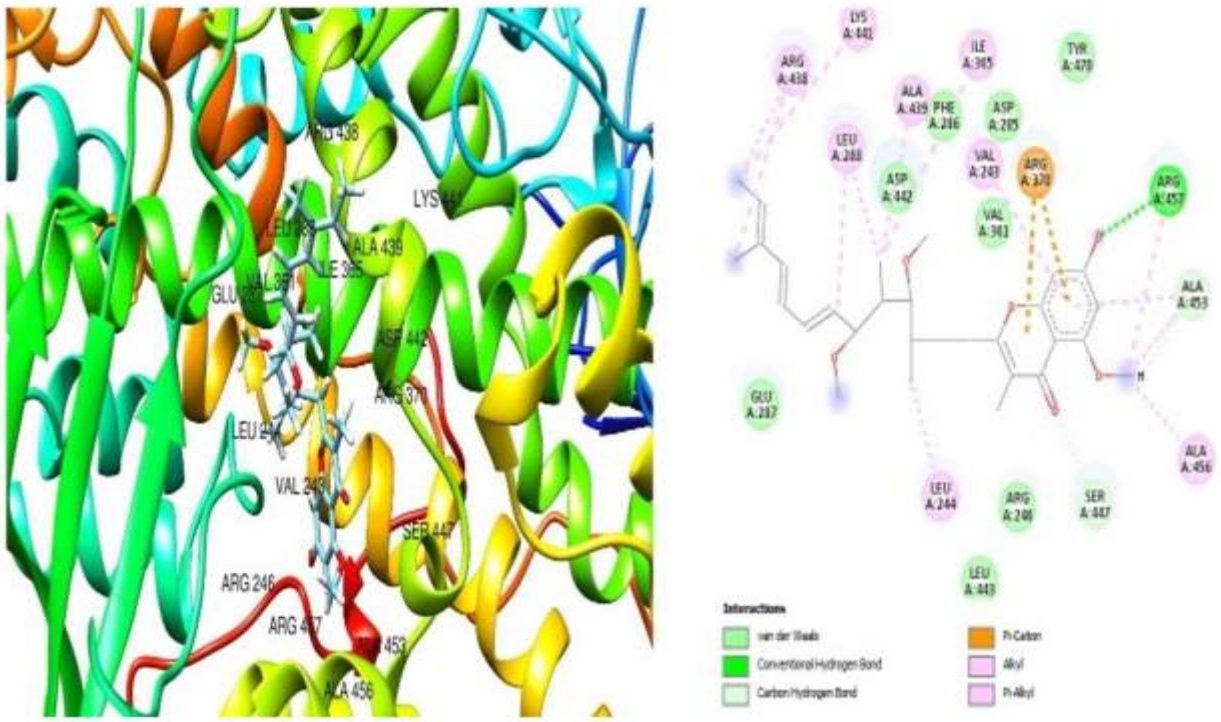


**Figure 7:** Molecular interaction of amino acids residues of 5-LOX (PDB ID: 3O8Y) with Stigmatellin Y (CID:5282078), 3D left, 2D right

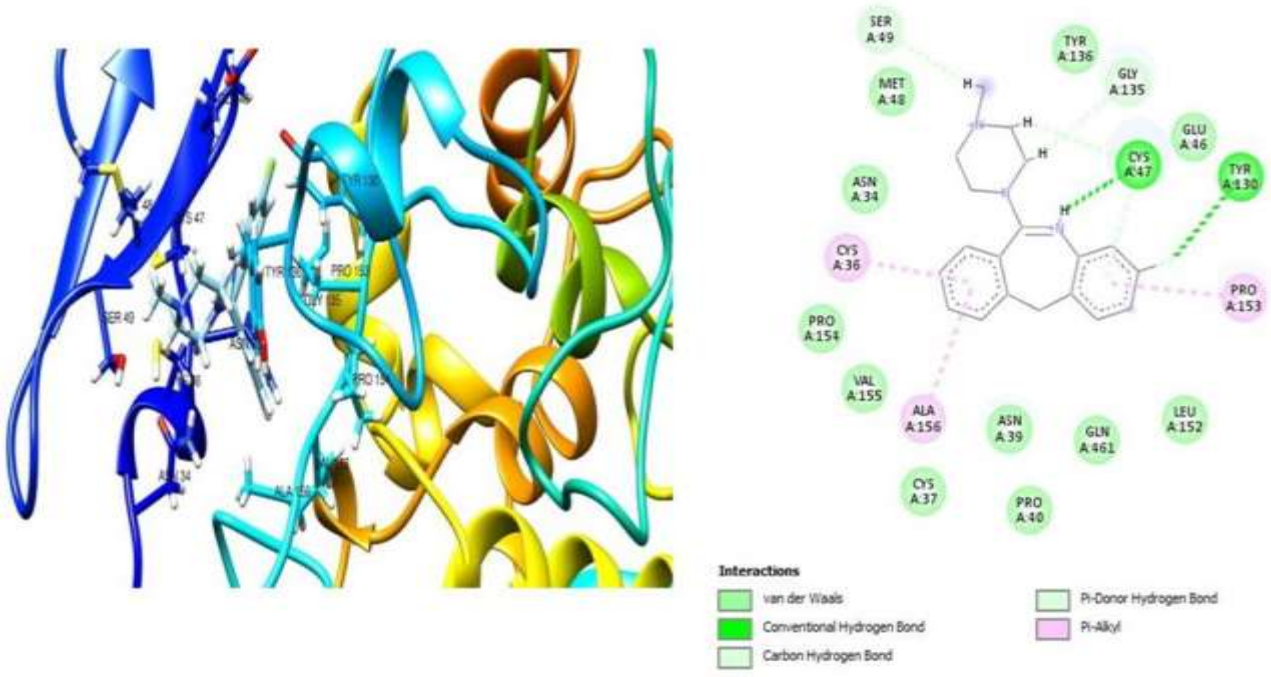


**Figure 8:** Molecular interaction of amino acids residues of OX (PDB ID: 1FIQ) with Fluperlapin (CID: 49381), 3D left, 2D right

ISSN 2616-0684 (Print)
ISSN 2616-0692 (Electronic)

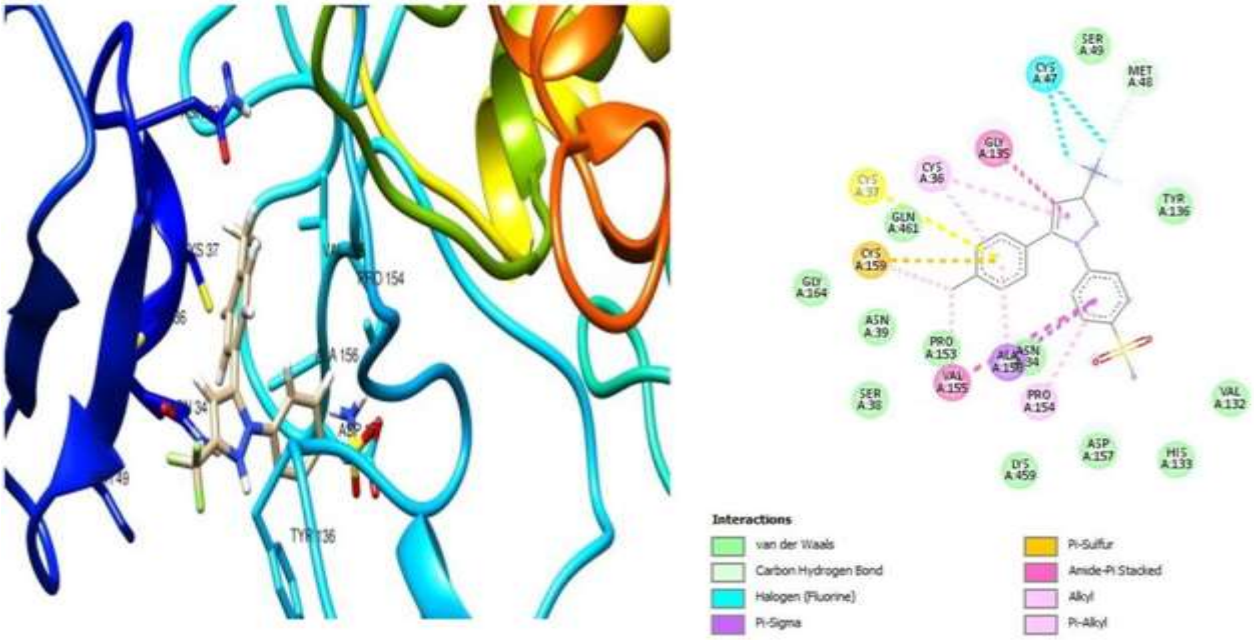


**Figure 9:** Molecular interaction of amino acids residues of COX-2 (PDB ID: 5W58) with Celecoxib (CID: 2662), 3D left, 2D right

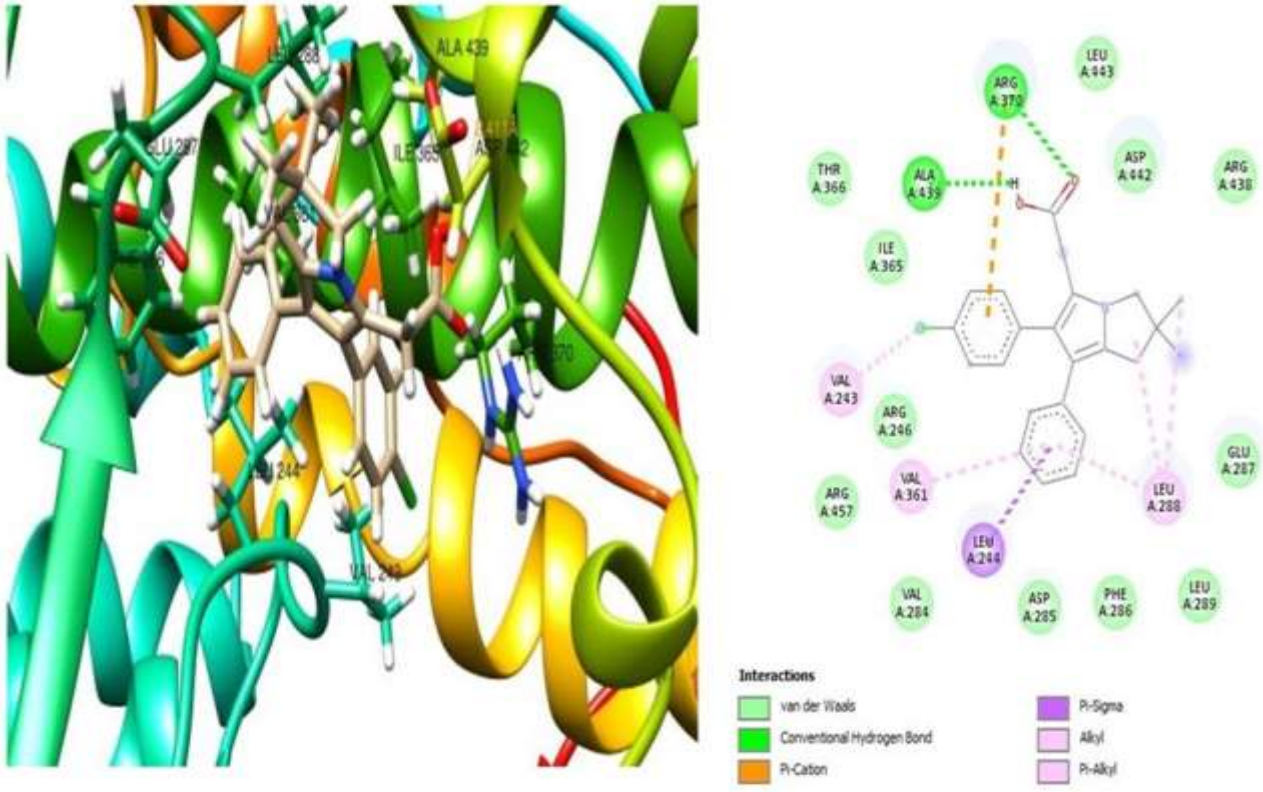


**Figure 10:** Molecular interaction of amino acids residues of 5-LOX (PDB ID: 3O8Y) with Licofelone (CID: 133021), 3D left, 2D right

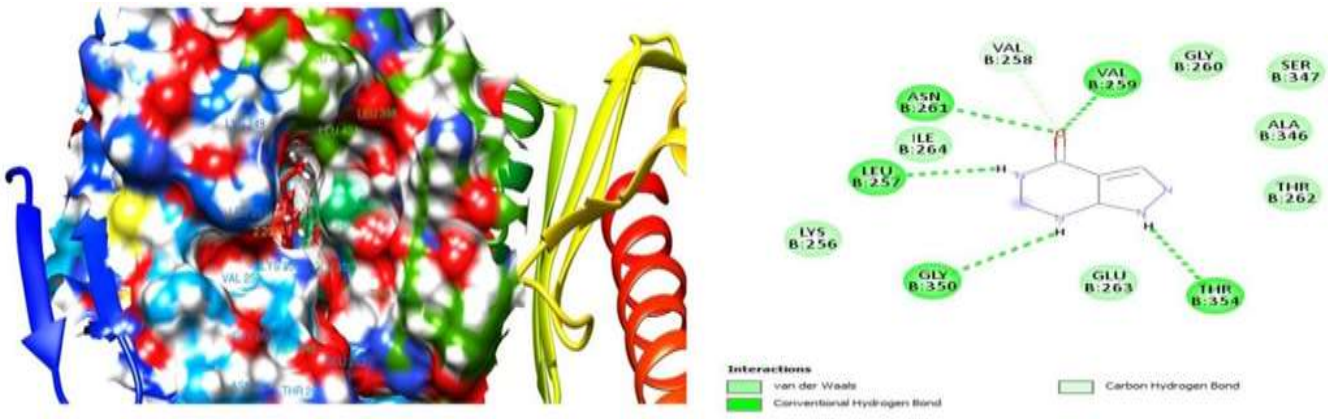


**Figure 11:** Molecular interaction of amino acids residues of OX (PDB ID: 1FIQ) with Allopurinol (CID: 135401907), 3D left, 2D right.

following non-covalent interactions: Van der Waals interactions with residues VAL 132, SER 38, ASN 157, GLY 164, carbon hydrogen bonding with GLN461 and PRO 153, π–alkyl interactions involving VAL155 and PRO154, π–sigma and amide–π stacking interactions with ALA158 and PRO154, π–sulfur interaction with CYS 37 and CYS 37, Halogen (fluorine) bonding contributing to added specificity. These diverse interactions, particularly the sulfonamide-linked π–sulfur and amide–π stacking, are essential for the selective inhibition of COX-2. The structure of COX-2 accommodates Celecoxib's side chains in a manner not possible in COX-1, thereby explaining its reduced gastrointestinal toxicity and COX-2 specificity. This binding mode aligns well with previous structural and pharmacological evidence supporting Celecoxib's role as a selective non-steroidal anti-inflammatory drug (NSAID).[32,33] Also, Figure 10 shows the summary of the molecular docking interaction between Licofelone (CID: 133021) and 5-lipoxygenase (5-LOX, PDB ID: 3O8Y). The 3D model reveals that Licofelone is deeply embedded within the binding cavity of 5-LOX, where it establishes significant interactions with key amino acid residues such as LEU 443, PHE 286, TYR 366 and ILE 365. These residues are spatially aligned to stabilize the Licofelone through various non-covalent interactions. In the 2D interaction, the following binding features were observed: Van der Waals interactions with residues including VAL 284, LEU 443, ASP 442, ARG 438, GLU 287, LEU 289, PHE 286, THR 366 and VAL 284, carbon hydrogen bonds with ARG 370 and ALA 439, which are critical for licofelone stabilization within the hydrophobic core, π–alkyl with LEU 288 and alkyl interactions with VAL 361 and VAL 243, further enhancing its binding strength. The result of this study supported the inhibitory activity of licofelone against 5-LOX evaluated during a clinical trial.[34] Figure 11 explains the molecular docking interaction of allopurinol (CID: 135401907) with xanthine oxidase (OX), using the crystal structure with PDB ID: 1FIQ. The left structure shows the three-dimensional (3D) binding orientation of allopurinol within the active site pocket of the protein, while the right structure depicts a two-dimensional (2D) schematic of specific amino acid interactions. The 3D model highlights the molecular environment surrounding the active site of XO. Allopurinol is shown docked firmly within the enzyme's binding pocket, surrounded by key residues that facilitate stable interactions. In the 2D interaction model (Figure 6, right), several non-covalent interactions are observed between allopurinol and the surrounding amino acids. Notably, conventional hydrogen bonds are formed with ASN 261, VAL 259, LEU 257, GLY 350, THR354 and carbon hydrogen interaction with ILE 264, which play critical roles in stabilizing the Allopurinol within the active site. Additional van der Waals interactions are observed with ILE 256, VAL 258, GLY 260, SER 347, ALA 346, THR 262, and GLU 263. These interactions collectively contribute to the binding affinity and specificity of allopurinol for xanthine oxidase. The nature and number of interactions suggest a strong binding affinity of allopurinol to xanthine oxidase, consistent with its known pharmacological role as a xanthine oxidase inhibitor.[35]This mechanism underlies its clinical application in the treatment of hyperuricemia and gout, where it effectively reduces the production of uric acid by inhibiting the oxidation of hypoxanthine and xanthine.[35]

## Conclusion

This study concluded that the PRF of SB leaf possesses bioactive phytoconstituents with significant anti-inflammatory activities. Fluperlapin, Stigmatellin Y and Methyl picraquassioside A fingerprinted in PRF may serve as promising natural alternatives for the management of inflammatory related diseases. These findings suggest that SB leaf could be a potent natural source of anti-inflammatory agents and may provide a therapeutic foundation for developing plant-based remedies. Further research should be conducted on the isolation and structural elucidation of the compounds identified in PRF. This will enhance the confirmation of their chemical identities and enable more precise pharmacological evaluation. Additionally, *in vivo* studies are recommended to unravel the exact molecular mechanisms underlying the anti-inflammatory activities of these compounds with a strong focus on COX-2, XO and 5-LOX.

## Conflict of Interest

The authors declare no conflict of interest.

## Author's Declaration

The authors hereby declare that the works presented in this article are original and that any liability for claims relating to the content of this article will be borne by them.

## Acknowledgements

The authors express their gratitude to Mr. Dayo of the Department of Biochemistry and Molecular Biology at Ile-Ife, Nigeria, and Mrs. Hassan Judith of the Department of Chemical Sciences at Dominion University of Ibadan, Nigeria, for their technical assistance in identifying and authenticating the plant. They also acknowledge the support of Mr. G.A. Ademoriyo of the Department of Botany at Obafemi Awolowo University in Ile-Ife, Nigeria.

## References

1. Karbab A, Mokhnache K, Ouhida S, Charef N, Djabi F, Arrar L, Mubarak MS. Anti-inflammatory, analgesic activity, and toxicity of *Pituranthos scoparius* stem extract: An ethnopharmacological study in rat and mouse models. J Ethnopharmacol. 2020; 258:112936.
2. Khelifi I, Hayouni EA, Cazaux S, Ksouri R, Bouajila J. Evaluation of *in vitro* biological activities: antioxidant; anti-inflammatory; anti-cholinesterase; anti-xanthine oxidase, anti-

superoxyde dismutase, anti-α-glucosidase and cytotoxic of 19 bioflavonoids. Cell Mol Biol. 2020;66(1):9-19.
3. Ajiboye BO. Molecular interaction of bioactive compounds from *Senecio biafrae* leaf with α-amylase and α-glucosidase receptors. Clin Phyt. 2022;8(1):4.
4. Baiyeri S. Proximate, minerals, vitamins, and antinutrients and their correlations in the leaves of *Senecio biafrae* accessions. J Agric Sci (Belgrade). 2023;68(1):67-79.
5. Lienou LL, Telefo PB, Rodrigues GQ, Donfack JN, Araújo RA, Bruno JB, Njimou JR, Mbemya TG, Santos RR, Souza JF, Figueiredo JR. Effect of different extracts and fractions of *Senecio biafrae* (Oliv. & Hiern) J. Moore on *in vivo* and *in vitro* parameters of folliculogenesis in experimental animals. J ethnopharmacol. 2020; 251:112571.
6. JO A, OV O, JT A, OE A, AF A, OO B. Brine shrimps' lethality test of ethanol extract and gas chromatography-mass spectrometry analysis of ethyl acetate fraction of *Blighia sapida*. Asian J Pharm Clin Res. 2020;13(8):208-212.
7. Sakulnarmrat K, Konczak I. Composition of native Australian herbs polyphenolic-rich fractions and *in vitro* inhibitory activities against key enzymes relevant to metabolic syndrome. Food Chem. 2012;134(2):1011-1119.
8. Singleton VL, Orthofer R, Lamuela-Raventos RM. Analysis of total phenols and other oxidation substrates and anti-oxidants by means of Folin-Ciocalteau reagent. Meth enzymol.1999;152-178.
9. Adeyemo AE, Omoba OS, Olagunju AI, Josiah SS. Assessment of nutritional values, phytochemical content, and antioxidant properties of Shallot (*Allium ascalonicum* L.) leaf and bulb. Measurement: Food. 2023; 10:1-9.
10. Adekola MB, Areola JO, Fagbohun OF, Asaolu FT, Ogundepo GE, Fajobi AO, Babalola OO. In-vitro antioxidant and anti-inflammatory activities of ethanol stem-bark extract of *Blighia sapida* KD Koenig. J Pharm Anal. 2022;12(2):350-354.
11. Sun PX, Yie LK, Zhang ZL, Hu M, Lu L. Colometric determination of the total content of the flavonoids in *Epimedium capsules*. J. Shenyang Pharm. Univ. 1999; 16:68-70.
12. Olarenwaju O, Apata JT, Akinpelu BO, Akomolafe RO, Oyemitan IA, Asaolu FT, Ologe MO, Iwalewa EO. Anti-inflammatory potentials, membrane stabilizing and xanthine oxidase inhibitory activities of *Clerodendrum volibule* ethanolic leaf extract on carragenaan-induced inflammation in rats. Int J Pharmacol Toxicol. 2018;6(1):7-11.
13. Nowacka-Jechalke N, Nowak R, Lemieszek MK, Rzeski W, Gawlik-Dziki U, Szpakowska N, Kaczyński Z. Promising potential of crude polysaccharides from *Sparassis crispa* against colon cancer: An in vitro study. Nutrients. 2021;13(1):161.
14. Lim MW, Yow YY, Gew LT. LC–MS profiling-based non-targeted secondary metabolite screening for deciphering cosmeceutical potential of Malaysian algae. J Cosmet Dermatol. 2023;22(10):2810-28
15. Johnson TO, Adegboyega AE, Iwaloye O, Eseola OA, Plass W, Afolabi B, Rotimi D, Ahmed EI, Albrakati A, Batiha GE, Adeyemi OS. Computational study of the therapeutic potentials of a new series of imidazole derivatives against SARS-CoV-2. J Pharmacol Sci. 2021;147(1): 62-71.
16. Bello O, Ayanda O, Aworunse O, Olukanmi B, Soladoye M, Esan E, Obembe O. *Solanecio biafrae:* An underutilized nutraceutically-important African indigenous vegetable. Pharmacog Rev. 2018;12(23): 128-132.
33. Ramsis T, Selim HM, Elseedy H, Fayed EA. The role of current synthetic and possible plant and marine phytochemical compounds in the treatment of acne. RSC Adv. 2024;14(33):24287-24321.
34. Apalowo RK, Chronopoulos D. A wave-based numerical scheme for damage detection and identification in two-dimensional composite structures. Comp str. 2019; 214:164-182.
35. Moreira J, Ribeiro D, Silva PM, Nazareth N, Monteiro M, Palmeira A, Saraiva L, Pinto M, Bousbaa H, Cidade H. New alkoxy flavone derivatives targeting caspases: Synthesis and antitumor activity evaluation. Mol. 2018;24(1):129.
17. Zhuang S, Yun H, Zhou X, Li Y, Li S, Liu C, Zhang Y. Screening, isolation, and activity evaluation of potential xanthine oxidase inhibitors in Poria Cum Radix Pini and mechanism of action in the treatment of gout disease. J Sep Sci. 2024;47(1):2300505.
18. Kumar S, Chopra B, Dass R, Dhingra AK. Health Benefits of Nutraceuticals in Gout Patients. In nutraceuticals and bone health, Apple Acad Press, 2024, pp. 175-190.
19. Suchitha GP, Devasahayam Arokia Balaya R, Prasad TS, Dagamajalu S. A signaling network map of Lipoxin (LXA4): an anti-inflammatory molecule. Inflam Res. 2024;73(7): 1099-1106.
20. Costa V, Costa M, Videira RA, Andrade PB, Paiva-Martins F. Anti-inflammatory activity of olive oil polyphenols—The role of oleacein and its metabolites. Biomed. 2022;10(11):2990.
21. Galvis CE, Kouznetsov VV. Recent advances for the C–C and C–N bond formation in the synthesis of 1-phenethyl-tetrahydroisoquinoline, aporphine, homoaporphine, and β-carboline alkaloids. Syn. 2017;49(20): 4535-4561.
22. Talib WH, Baban MM, Azzam AO, Issa JJ, Ali AY, AlSuwais AK, Allala S, Al Kury LT. Allicin and Cancer Hallmarks. Mol. 2024;29(6):1320.
23. Zhang S, Mao B, Cui S, Zhang Q, Zhao J, Tang X, Chen W. Absorption, metabolism, bioactivity, and biotransformation of epigallocatechin gallate. Crit Rev Food Sci and Nutr. 2024;64(19): 6546-6566.
24. Nunes CD, Barreto Arantes M, Menezes de Faria Pereira S, Leandro da Cruz L, de Souza Passos M, Pereira de Moraes L, Vieira IJ, Barros de Oliveira D. Plants as sources of anti-inflammatory agents. Mol. 2020;25(16): 3726.
25. John A, Rusted J, Richards M, Gaysina D. Accumulation of affective symptoms and midlife cognitive function: the role of inflammation. Brain, Behav Immun. 2020; 84:164-172.
26. Mahboubi-Rabbani M, Abdolghaffari AH, Ghesmati M, Amini A, Zarghi A. Selective COX-2 inhibitors as anticancer agents: a patent review (2018-2023). Expt Opin Therap. Patents. 2024;34(9):733-757.
27. Szczukowski Ł, Krzyżak E, Zborowska A, Zając P, Potyrak K, Peregrym K, Wiatrak B, Marciniak A, Świątek P. Design, synthesis and comprehensive investigations of pyrrolo [3, 4-d] pyridazinone-based 1, 3, 4-oxadiazole as new class of selective cox-2 inhibitors. Int J Mol Sci. 2020;21(24): 9623.
28. Desind SZ, Bell SK, Davidson ZM, Lutz CS. Long noncoding RNAs and their complex role in shaping and regulating arachidonic acid metabolism: Learning to love the (not-really) junk. Wiley Int Rev: RNA. 2024;15(1): e1828.
29. Wautier JL, Wautier MP. Pro-and anti-inflammatory prostaglandins and cytokines in humans: a mini review. Int J Mol Sci. 2023;24(11): 9647.
30. Kulkarni A, Nadler JL, Mirmira RG, Casimiro I. Regulation of tissue inflammation by 12-lipoxygenases. Biomol. 2021;11(5): 717.
31. Houglum JE, Harrelson GL, Seefeldt TM. Drugs for treating inflammation. In Principles of Pharmacology for Athletic Trainers, Routledge. 2024, pp. 96-123.
32. Karagiannis TC, Ververis K, Liang JJ, Pitsillou E, Kagarakis EA, Yi DT, Xu V, Hung A, El-Osta A. Investigation of the Anti-Inflammatory Properties of Bioactive Compounds from *Olea europaea*: In Silico Evaluation of Cyclooxygenase Enzyme Inhibition and Pharmacokinetic Profiling. Mol. 2024;29(15):3502.